Preprint 25th EU PVSEC / WCPEC-5 Valencia 2010

TIME RESOLVED PHOTOLUMINESCENCE IMAGING FOR CARRIER LIFETIME MAPPING OF SILICON WAFERS

D. Kiliani, G. Micard, B. Raabe, G. Hahn
University of Konstanz, Department of Physics,
78457 Konstanz, Germany

ABSTRACT: A method for time-resolved Photoluminescence Imaging using a high-resolution Si-CCD camera was developed. The use of a fast rotating shutter wheel decouples the obtained temporal resolution from the camera exposure time, making it possible to record the decay curve of free minority charge carriers. With this transient measurement, maps of the effective carrier lifetime can be generated for different carrier densities without the use of external calibration measurements.
Keywords: Experimental Methods, Lifetime, Photoluminescence

1 INTRODUCTION

The determination of charge carrier lifetimes is an important task in the development of higher solar cell efficiencies. It may be used to quantify the quality of bulk material for solar cell production, as well as surface passivation techniques applied to silicon wafers. Especially with regard to multicrystalline silicon solar cells, spatially resolved methods to measure the effective lifetime of excited minority charge carriers play an important role in the development and production of high-efficiency solar cells. In contrast to integral methods like quasi-steady-state photoconductance (QSSPC) [1] and photoluminescence (QSSPL) [2], they allow the determination of lateral lifetime variations, e.g. caused by inhomogeneous surface passivation or the aggregation of impurities in grain boundaries.

Typical methods for spatially resolved lifetime measurement in solar cell development are microwave-detected photoconductance decay (MWPCD) [3], thermal radiation absorption (CDI/ILM) [4] and photo-luminescence imaging (PLI) [5]. MWPCD is a dynamic raster method, where the effective lifetime is determined from the carrier decay transient curve for each point of the sample. It is therefore much slower than the camera-based methods CDI and PLI, which record a signal corresponding to the charge carrier density under steady-state illumination in one shot for the whole sample. These steady-state methods do, however, have the disadvantage to require an exact calibration of the corellation function between radiation intensity and charge carrier density, which is usually done with the integral methods QSSPC or QSSPL [6]. This approach works well when the excitation and emissivity of the sample are homogeneous, but does not account for lateral variations of the calibration function, which may e.g. be caused by light reflections or surface texture.

Ramspeck et al. [7] have recently demonstrated a method for camera-based dynamic ILM lifetime measurements which does not require external calibration. It uses very short exposure times in the region of the carrier lifetime in the sample, which are possible due to the high intensity of the recorded thermal radiation and the electronic shuttering of the camera. Using a standard Si-CCD camera for photoluminescence imaging, this approach is not feasible due to the slower camera readout times and the need of an external shutter during readout. Nevertheless, a dynamic method using PLI was deemed rewarding due to the higher resolution and lower equipment cost of silicon CCD cameras. This was achieved by installing a rotating shutter wheel in front of the camera lens [8].

2 MEASUREMENT SETUP

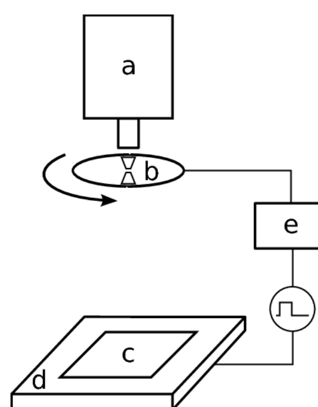

Figure 1: Schematic layout of the measurement setup. The camera (a) looks through the shutter wheel (b) at the sample (c), which is illuminated by an LED panel (d).

A layout of the measurement setup for time-resolved photoluminescence imaging (TR-PLI) is shown in Figure 1. We used a standard PLI setup with a silicon CCD camera (a) and added a rotating shutter wheel in front of the objective lens. The shutter wheel has sectoral slits, which uncover the lens for short periods of time. The sample (c) is placed beneath the camera on an LED panel (d) and illuminated homogeneously from below. The LED panel emits a fixed photon flux of $E = 5.0 \times 10^{17}$ cm^{-2}s^{-1} – about 2 suns equivalent – and can be switched on and off by an excitation control box (e). The shutter wheel is driven by a brushless DC motor so the excitation controller can synchronize the LED panel to its rotation with an adjustable phase delay.

The sample is therefore periodically illuminated for 50% of the period length T, while the shutter wheel slits always uncover the lens at a defined phase of this excitation cycle. This allows for a decoupling of the CCD exposure time and the temporal resolution of the measurement, which is determined by the time for one slit to pass in front of the lens and therefore is much shorter. By changing the rotation speed of the shutter wheel, excitation periods between 1 and 10 ms are possible to obtain optimal time-resolution for samples of different effective lifetime. The excitation phase has to be long enough for all regions of the sample to reach the maximum charge carrier density Δn_0 as under steady-state illumination.

For the actual measurement, several PL images are recorded for different phase delays φ around the falling

flank of the signal curve (see Figure 3) and normalized using the steady-state PL image.

3 EVALUATION

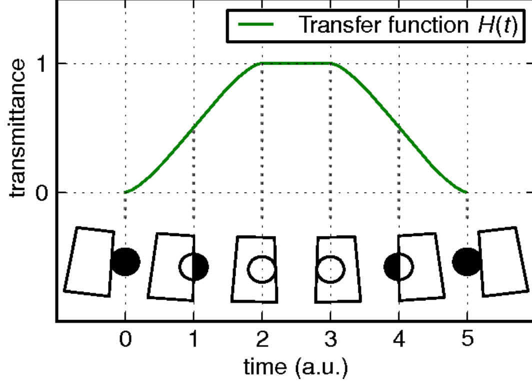

Figure 2: Transfer function of the shutter wheel. The visible aperture area of the circular objective lens varies during the depicted exposure process.

The exposure process of the CCD chip during one excitation cycle is determined by the transfer function H(t) of the shutter wheel (Figure 2). The slopes of H(t) are given by integration over the circular lens aperture area:

$$A(\alpha) = \frac{2}{\pi}\int_0^\alpha \sqrt{1-x^2}\,dx + \frac{1}{2}.$$

The plateau in the middle of H(t) occurs when the size of the lens aperture is smaller than the shutter wheel slit.

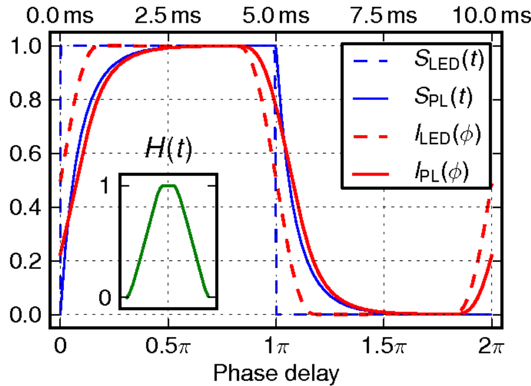

Figure 3: Original signals S(t) (blue) and convolved intensities I(φ) as seen by the camera (red). The dashed lines show the LED signal, the solid lines the photoluminescence of a sample with τ_{eff} = 530 ms.

As shown in Figure 3, the camera intensity for a given phase shift φ is then given by the convolution of the time-dependant PL signal with the transfer function H(t):

$$I(\phi) = \int_0^T S(t + T\frac{\phi}{2\pi})H(t)dt$$

The camera signal I(φ) is effectively blurred by H(t), a process which cannot be easily be reversed e.g. by deconvolution. The shape of H and the noise in the camera data lead to strong oscillations in the deconvoluted signal, making it unusable for lifetime calculation. But as the shape of the LED signal $S_{LED}(t)$ is known to be rectangular and the convolved signal $I_{LED}(\varphi)$ can be measured, the parameters of H(t) can be estimated by fitting the convolved step function – which is the integral of H – to the measured I_{LED}. When H(t) is determined quantitatively, the camera intensity for arbitrary signals can be calculated by numerical convolution.

In order to extract lifetime values by fitting convolved decay curves to the measured data, a parametric model for the decay of excited minority charge carriers was developed. It is based on the nonlinear differential equation

$$\frac{d\Delta n}{dt} = -C\Delta n - D(\Delta n)^2,$$

which uses only the linear and quadratic terms in Δn, so the differential equation is still analytically solvable. The solution

$$\Delta n(t) = \frac{C}{(C/\Delta n_0 + D)e^{Ct} - D}$$

depends only on the coefficients C and D, and the initial excess charge carrier density Δn_0 at t = 0. From this solution, the time-dependant PL signal S(t) can be calculated, using the rate of radiative recombination

$$\Phi(\Delta n) = B\,\Delta n(N + \Delta n).$$

N is the doping concentration and B is the constant of radiative recombination in silicon, which is constant except for high values of Δn [9]. The normalized PL decay is therefore given by

$$S(\frac{T}{2} + t) = \frac{B(\Delta n(t))\,\Delta n(t)(N + \Delta n(t))}{B(\Delta n_0)\,\Delta n_0(N + \Delta n_0)}.$$

When the two parameters C and D of the model have been determined from the fit, they can be used to calculate effective excess charge carrier lifetimes τ_{eff} from the slope of Δn

$$\tau_{eff}(\Delta n) = -\Delta n(t)/\frac{d\Delta n(t)}{dt} = \frac{1}{C + D\Delta n}.$$

From this expression we see that the approach yields a lifetime of 1/C, which is decreased by the quadratic term for high carrier densities when DΔn becomes significant.

The initial charge carrier density Δn_0 can be estimated in the fitting process from the LED light intensity E via

$$\Delta n_0 = \frac{\tau_{eff}(\Delta n_0)\,E\,(1 - R)}{w},$$

where w is the thickness and R the reflectivity of the sample.

4 RESULTS

Lifetime measurements of different silicon wafers were successfully performed with the presented method. The sample shown in the following is a 5 cm wide p-type FZ-Si wafer with a resistivity of 2 Ωcm and a thickness of 525 µm. Both surfaces have a high quality Al_2O_3 passivation, resulting in an effective lifetime of ≈ 4 ms at $\Delta n = 10^{15}$ cm^{-3} in the middle of the sample. Due to the fixed intensity of the LED panel in the current setup, Δn_0 for TR-PLI measurements is much higher, about 9×10^{15} cm^{-3} in the center of the sample. The TR-PLI lifetime map in Figure 4a shows the sample at Δn_0, where the values of τ_{eff} are significantly lower than in the second lifetime map (b), calculated at 0.5 Δn_0. The TR-PLI lifetime maps agree very well with the steady-state PL image, shown in Figure 5. In both images, areas of lower lifetime at the wafer edges can be seen, caused by

handling of the sample in different steps of the surface passivation process. A notable difference between the steady-state PL image and the TR-PLI lifetime maps can be seen in the center of the sample. The PL image has a square area of higher intensity, which is caused by reflected light. As the TR-PLI method does not depend on absolute intensities, this artifact does not occur in the lifetime maps in Figure 4.

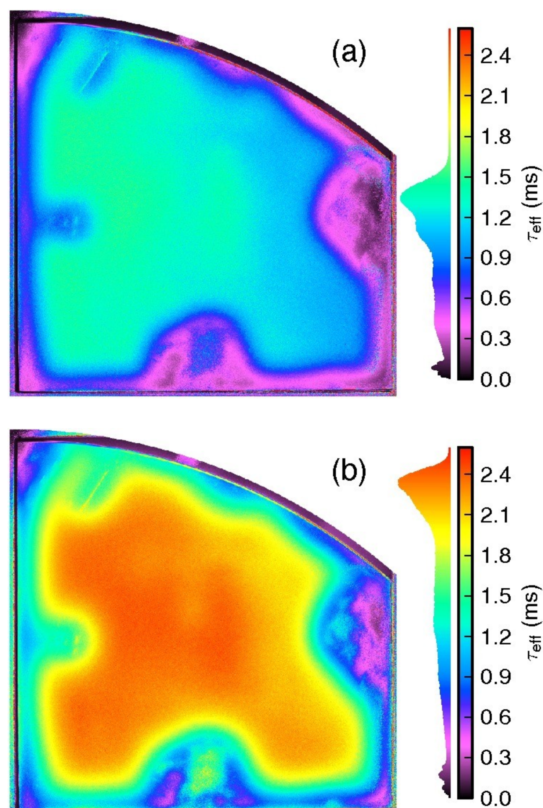

Figure 4: TR-PLI lifetime maps of an Al_2O_3 passivated FZ-Si wafer, measured at Δn_0 (a) and 0.5 Δn_0 (b).

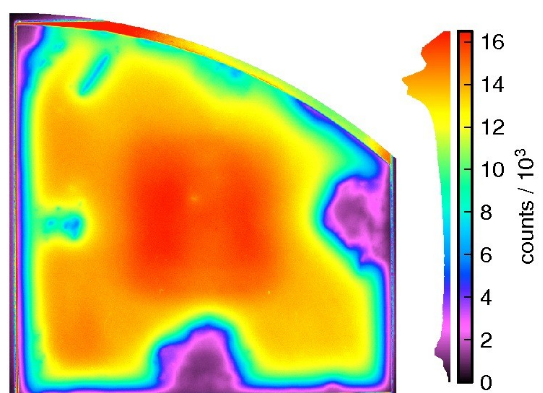

Figure 5: Steady-state PL image of the sample shown in Figure 4.

The effective lifetime values were also compared with a transient photoconductance measurement in the center of the sample. The resulting lifetime curves (Figure 6) show very good agreement, with a small discrepancy for lower values of Δn. This can be explained by the higher relative fitting error in this region and the fact that the carrier density model has only two parameters and cannot perfectly describe the actual transient curve. To record the effective lifetime over a wider range of Δn, several measurements with varying LED intensity have to be recorded and can be combined.

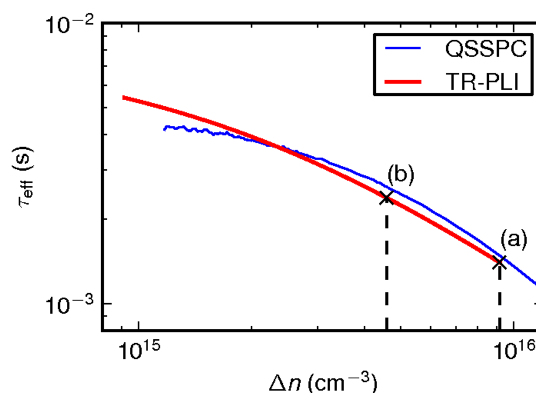

Figure 6: Effective lifetime from photoconductance measurement and TR-PLI for the center of the sample shown in Figure 4.

5 CONCLUSION

A method to record and evaluate time-resolved photoluminescence images of crystalline silicon wafers using a standard Si-CCD camera was developed. The transient curve for each pixel is determined from a set of PL images, making the method calibration-free and much faster than MWPCD measurements. Lifetime maps for different injection levels can be calculated and show good agreement with steady-state PL images and QSSPC measurements. Compared with the dynamic ILM/CDI method, a higher spatial resolution at much lower equipment cost can be obtained.

6 ACKNOWLEDGEMENTS

We would like to thank Thomas Lüder for providing the sample shown in this talk and the German BMU for funding provided under contract number 325033.

7 REFERENCES

[1] R. Sinton, A. Cuevas and M. Stuckings, Proc. 25th IEEE PVSC, Washington (1996)

[2] T. Trupke and R.A. Bardos, Proc. 31st IEEE PVSC, Orlando (2005)

[3] J. Schmidt and A. G. Aberle, J. Appl. Phys. 81, 6186 (1997)

[4] S. Riepe, J. Isenberg, C. Ballif, S.W. Glunz and W. Warta, Proc. 17th EUPVSEC, Munich (2001)

[5] T. Trupke, R.A. Bardos, M.C. Schubert and W. Warta, Appl. Phys. Lett. 89, 44107 (2006)

[6] S. Herlufsen, J. Schmidt, D. Hinken, K. Bothe and R. Brendel, physica status solidi (RRL) 2, 245 (2008)

[7] K. Ramspeck, S. Reissenweber, J. Schmidt, K. Bothe and R. Brendel, Appl. Phys. Lett. 93, 102104

(2008)

[8] D. Kiliani, G. Micard, B. Raabe, G. Hahn, submitted to Appl. Phys. Lett. (2010)

[9] P.P. Altermatt, F. Geelhaar, T. Trupke, X. Dai, A. Neisser and E. Daub, Appl. Phys. Lett. 88, 261901 (2006)